Available online at www.sciencedirect.com
SCIENCE DIRECT
Physics Letters A 348 (2006) 195–200
PHYSICS LETTERS A
www.elsevier.com/locate/pla

Chaotic attractors in striped rectangular shapes generated by a Rössler-like system ☆

Qingfei Chen [a], Yiguang Hong [b,*], Guanrong Chen [c], Qiuhai Zhong [a]

[a] *Department of Automatic Control, Beijing Institute of Technology, Beijing, China*
[b] *Key Laboratory of Systems and Control, Institute of Systems Science, Chinese Academy of Sciences, Beijing, China*
[c] *Department of Electronic Engineering, City University of Hong Kong, Hong Kong, China*

Received 19 April 2005; received in revised form 7 August 2005; accepted 9 August 2005

Available online 6 September 2005

Communicated by C.R. Doering

Abstract

This Letter introduces some new chaotic attractors in striped rectangular shapes. The chaotic attractors are constructed by adding bounded and non-smooth feedback control to the Rössler system. The shape of a generated chaotic attractor can be adjusted by changing some control parameters. Moreover, the dynamical behavior of the considered system is investigated and some estimations for characteristics of this attractor are given.

Chaotic dynamics and chaos control have been investigated in the last four decades [1–3], with many chaotic attractors such as Lorenz attractor [4] and Rössler attractor [5] found.

Lately, from engineering viewpoints, by circuit implementation and feedback control technique, more chaotic attractors were generated (for example, Chua's circuit [6] and Chen's system [7]). Using feedback control technique to generate new chaotic attractors is called anti-control of chaos [1], which can be quite effective in increasing the complexity of the original dynamic system. Existing works have shown that even a simple feedback control mechanism can generate a variety of chaotic attractors with different structures having, for example, multi-scrolls [8], or butterfly-shapes [9].

The motivation of this Letter also follows the idea of controlling a dynamical system to generate special patterns so as to meet some design specifications. Here, a new kind of chaotic attractors in striped rectangular forms are generated via control from the Rössler systems. The created chaotic attractors consist of quite "unusual" multiple stripes in rectangular

☆ This work was supported by the NNSF of China under Grants 60425307, 10472129 and 10475009.

* Corresponding author.
E-mail address: yghong@iss.ac.cn (Y. Hong).

0375-9601/$ – see front matter
doi:10.1016/j.physleta.2005.08.085

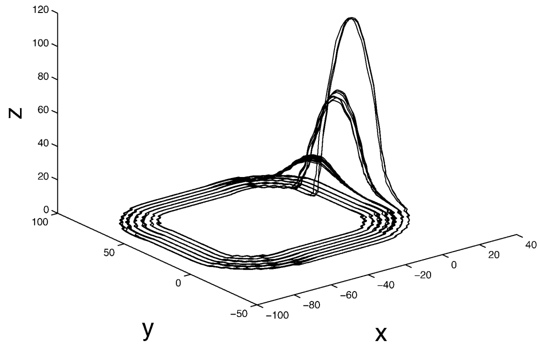

Fig. 1. The system orbit generated by (1).

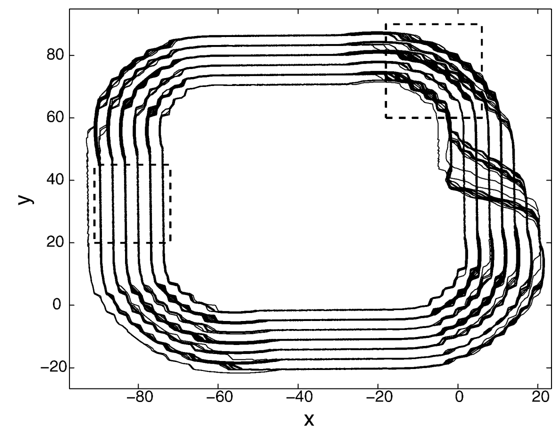

Fig. 2. x–y projection of the attractor of Fig. 1.

shapes. The shape and size of an attractor can be well controlled by adjusting some system parameters.

Here, we consider a Rössler-like system:

$$\begin{cases} \dot{x} = -(y+z) + \epsilon_1(f + \mathrm{rec}(ex)), \\ \dot{y} = x + ay + \epsilon_2(f + \mathrm{rec}(ey)), \\ \dot{z} = z(x-c) + b, \end{cases} \tag{1}$$

which can be viewed as the well-known Rössler system with added feedback control inputs $\epsilon_1(f + \mathrm{rec}(ex))$ and $\epsilon_2(f + \mathrm{rec}(ey))$, where $\mathrm{rec}(\cdot)$ is a rectangular wave generating function described as follows:

$$\mathrm{rec}(x) = \begin{cases} 1 & 2k\pi \leqslant x < 2k\pi + \pi, \\ 0 & 2k\pi + \pi \leqslant x < 2k\pi + 2\pi. \end{cases}$$

Here $\epsilon_i \geqslant 0$, $i = 1, 2$ are the control gains, and $e > 0$ (representing the frequency of a periodic wave), and $f \geqslant 0$ (describing a constant translation) are "control" parameters.

Because the two feedback controllers in the first and second equations are bounded, they play a very little role when x, y, z are sufficiently large. Clearly, they could not spoil the existence of the generated attractor, which roots in the unforced Rössler system. Moreover, system (1) is by nature a non-smooth system, with switching planes located at $\{(x, y, z) | ex = k\pi,\ k = 0, \pm 1, \pm 2, \ldots\}$ and $\{(x, y, z) | ey = k\pi,\ k = 0, \pm 1, \pm 2, \ldots\}$.

Fig. 1 shows that system (1) generates a chaotic attractor of a striped rectangular shape, by taking the system parameters

$$a = 0.05, \qquad b = 0.20, \qquad c = 10.0, \tag{2}$$

and the "control" parameter as

$$e = 2, \qquad f = 0.4, \qquad \epsilon_1 = \epsilon_2 = 40. \tag{3}$$

Both Euler method and Runge–Kutta method have been used in the numerical studies. The numeral results with the two methods are almost the same. In what follows, the simulation results are obtained using Runge–Kutta method with the step length taken as 0.01. This new attractor seems quite different from most well-known chaotic attractors: it consists of several parallel stripes and the distance between two adjacent stripes is almost a constant; it is in the forms of a group of "rectangles" (not in the form of circles). It seems quite regular and simple if one only takes a quick glance at Fig. 2. However, if one checks it carefully, its intrinsic complex behavior can be found as illustrated in Fig. 3.

The maximum Lyapunov exponent (MLE) is very useful in the study of chaotic dynamics. However, for a non-smooth system, the calculation of MLE is not straightforward. Recently, some estimation methods of MLE for non-smooth dynamical systems have been reported in some papers such as [10,11]. Here, with parameters setting (2) and (3), the estimation of MLE of system (1) with the method given in [10] is 0.0282, while that with the method presented in [11] is 0.0234. Because both the estimated values of MLE are positive, the considered attractor is actually irregular and chaotic. In fact, the chaotic behaviors are hidden in the "regular" stripes.

The amplitudes of trajectories $x(t)$, $y(t)$ and $z(t)$ are roughly classified into several distinguishable levels, according to the "regularity" of the stripes. Take $z(t)$ as an example. The values of its amplitudes belong to three separated intervals; that is, [0, 2],

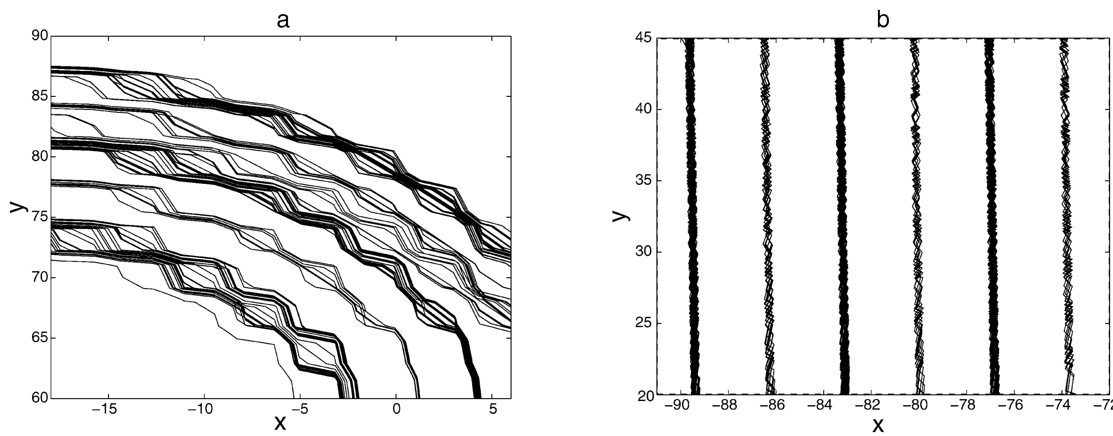

Fig. 3. Two enlarged parts in the dashed boxes of the first figure of Fig. 2.

[10, 20], and [45, 65], as shown in Fig. 4. In addition, $z(t)$ evolves intermittently.

Now let us consider the relationships between the characteristics of the generated chaotic attractors and the "control" parameters f, e, ϵ_1, and ϵ_2.

It can be seen that $z(t)$ of the attractor generated by system (1) stays near zero most of the time when the attractor moves in the regular "straight-line" orbit. To simplify the analysis, assume that $z \approx 0$ and $\dot{z} \approx 0$ roughly hold in most of the "straight-line" parts of the attractor of system (1). Then, system (1) approximatively reduces to:

$$\begin{cases} \dot{x} \approx -y + \epsilon_1(f + \mathrm{rec}(ex)), \\ \dot{y} \approx x + ay + \epsilon_2(f + \mathrm{rec}(ey)) \\ \text{when } \dot{z} \approx 0, z \approx 0. \end{cases} \tag{4}$$

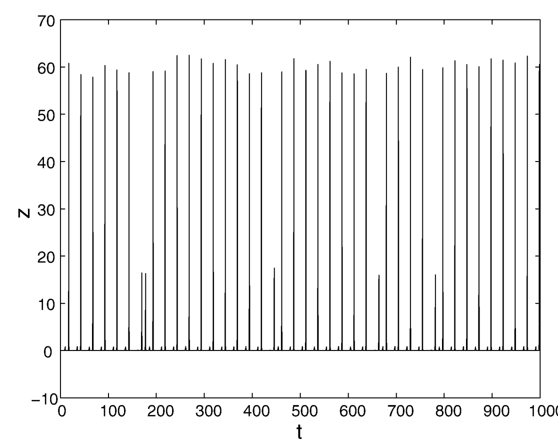

Fig. 4. Time series of $z(t)$ of system (1).

When the trajectory in the attractors moves along the straight-line part of an stripe paralleled with axis y, $\dot{x} \approx 0$. Then, from (4),

$$y \approx \epsilon_1\big(f + \mathrm{rec}(ex)\big). \tag{5}$$

Because the range of function $\epsilon_1(f + \mathrm{rec}(ex))$ is $[\epsilon_1 f, \epsilon_1(1 + f)]$, the "straight-line" orbit may be maintained between $y = \epsilon_1 f$ and $y = \epsilon_1(1 + f)$ in general. In other words, when the stripes of the attractor take the form of straight lines parallel to axis y, owing to $\dot{x} \approx 0$, they mainly appear in an interval with $y \in [\epsilon_1 f, \epsilon_1(1 + f)]$. Therefore, the length of the straight-line part of the stripes (of the left edge in the "rectangular" form) parallel to axis y is approximately ϵ_1. A larger value of ϵ_1 produces longer straight-line stripes parallel to axis y. However, when $\epsilon_1 = 0$, the lengths of the straight-line parts of the stripes parallel to axis y becomes 0; namely, the stripes are no longer paralleled to axis y, as shown Fig. 5 with (2) and $e = 3$, $f = 0.4$, $\epsilon_1 = 0$, $\epsilon_2 = 40$. On the other hand, as for the right edge of the "rectangular" form, $z(t)$ is not around 0, the above analysis based on the assumption of $z \approx 0$ is not valid.

Similarly, take $\dot{y} \approx 0$ to describe the straight-line orbit in the attractor parallel to axis x. Then, from (4), we have

$$x \approx -ay - \epsilon_2\big(f + \mathrm{rec}(ey)\big). \tag{6}$$

As a result, x is roughly in $[-\epsilon_2(1 + f) - ay, -\epsilon_2 f - ay]$ with y as the coordinates of certain stripes par-

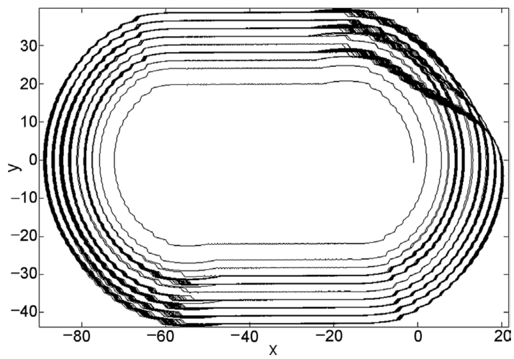

Fig. 5. x–y projection of the attractor with $\epsilon_1 = 0$.

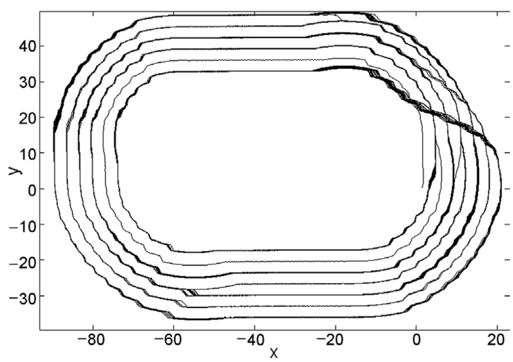

Fig. 6. x–y projection of the attractor with $\epsilon_1 = 10$.

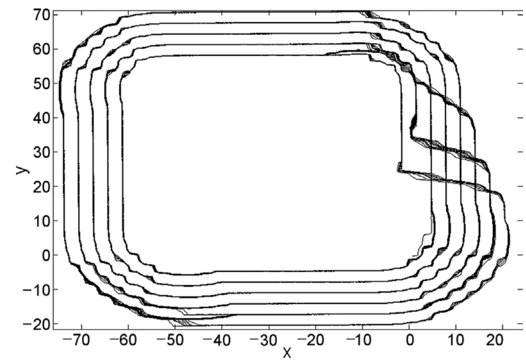

Fig. 7. x–y projection of the attractor with $f = 0.2$.

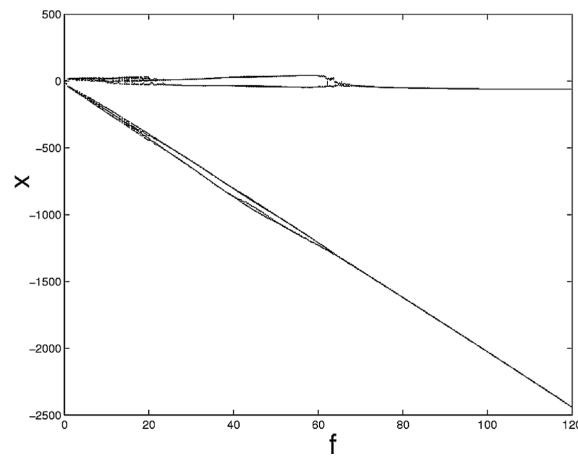

Fig. 8. Bifurcation diagram with parameter f.

allel to axis x. Therefore, the length of the straight-line parts of the stripes parallel to axis x is approximately ϵ_2.

Based on the above analysis, the ranges of straight lines in the attractors directly depend on the selection of ϵ_i $(i = 1, 2)$ and f. For example, we consider the change of the strength ϵ_1 with fixing (2), $e = 2$, $f = 0.4$, and $\epsilon_2 = 40$. Figs. 6 and 2 illustrate the cases with $\epsilon_1 = 10$ and $\epsilon_1 = 40$, respectively. Therefore, the ranges for the stripes in the form of straight lines parallel to axis y are, respectively, $y \in [4, 14]$ (when $\epsilon_1 = 10$), $y \in [16, 56]$ (when $\epsilon_1 = 40$), which are consistent with (5).

It is now to analyze the influence of f on the dynamics. By fixing (2), $\epsilon_1 = \epsilon_2 = 40$, and $e = 2$, Figs. 7 and 2 show the attractors of system (1) with $f = 0.2$ and $f = 0.4$, respectively. The ranges for the stripes in the form of straight lines parallel to axis y are, respectively, $y \in [8, 48]$ (when $f = 0.2$), $y \in [16, 56]$ (when $f = 0.4$). Furthermore, fix (2), $\epsilon_1 = 0, \epsilon_2 = 10$, and $e = 4$, and a bifurcation diagram (x vs. f) based on a Poincaré map with a cross section $\Sigma_1 = \{(x, y, z)^T \in R^3 \mid y = 0\}$ is shown in Fig. 8. There are two main branches. Fig. 9 shows some details for the upper branch of Fig. 8, where $B_f \approx 68$ is a bifurcation value.

Then, the role of e is investigated. Since $\mathrm{rec}(ex)$ is a function of period $2\pi/e$, its keeps the right-hand side of the first equation unchanged when x moves to $x \pm 2\pi/e$. Similar discussion can be given to $\mathrm{rec}(ey)$. Therefore, one may guess that, if these parallel stripes exist, the distance between those stipes can be estimated as $D = 2\pi/e$. In this sense, e is a parameter that directly affects the inter-stripe distance. Setting (2) and $\epsilon_1 = \epsilon_2 = 40$, $f = 0.4$, Figs. 2 and 10 demonstrate the attractors of system (1) with $e = 2$ and $e = 4$, respectively. Moreover, Fig. 11 illustrates a bifurcation diagram with parameter e based on a Poincaré map with

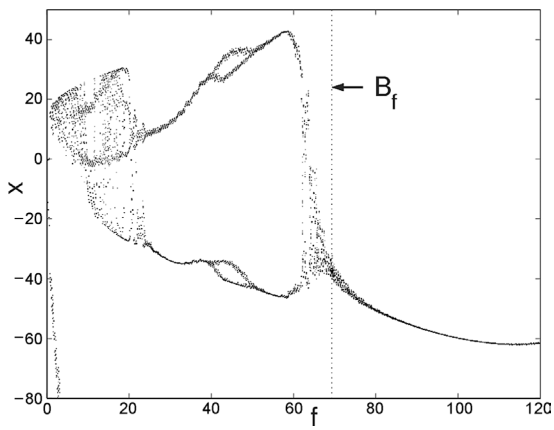

Fig. 9. The upper bifurcation branch.

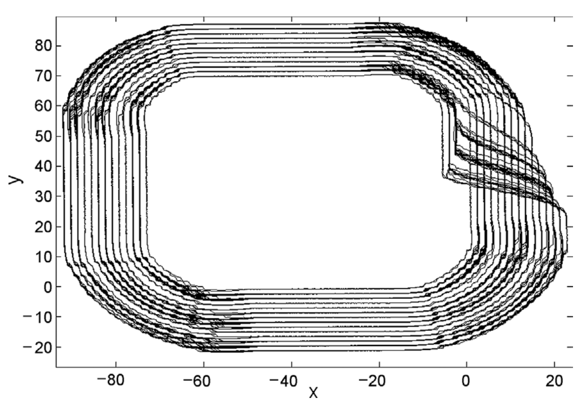

Fig. 10. x–y projection of the attractor with $e = 4$.

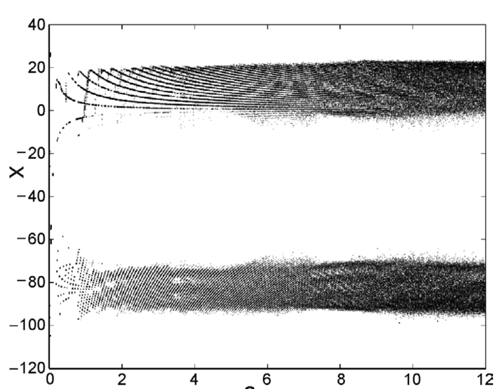

Fig. 11. Bifurcation diagram with parameter e.

surface $\Sigma_2 = \{(x, y, z)^T \in R^3 \mid y = 30\}$ (as discussed, with the chosen parameters, taking $y = 30 \in [16, 56]$ for Σ_2 ensures that the stripes parallel to axis y cross Σ_2 transversely). In addition to the comparison between Figs. 2 and 10, Fig. 11 also shows that an increasing e is narrowing the inter-stripe distance.

Finally, the equilibria and their stability of system (1) are discussed. Set

$$\Delta_1(t) = \begin{cases} \epsilon_1(f+1) & \text{if } \sin(ex) \geqslant 0, \\ \epsilon_1 f & \text{if } \sin(ex) < 0, \end{cases} \tag{7}$$

and

$$\Delta_2(t) = \begin{cases} \epsilon_2(f+1) & \text{if } \sin(ey) \geqslant 0, \\ \epsilon_2 f & \text{if } \sin(ey) < 0. \end{cases} \tag{8}$$

Then, system (1) can be rewritten as

$$\begin{cases} \dot{x} = -(y+z) + \Delta_1, \\ \dot{y} = x + ay + \Delta_2, \\ \dot{z} = z(x-c) + b. \end{cases} \tag{9}$$

The equilibria of system (9) can be easily obtained by solving the equations $\dot{x} = \dot{y} = \dot{z} = 0$. Therefore, if

$$(\Delta_2 + c + a\Delta_1)^2 - 4ab \geqslant 0,$$

then system (9) has two groups of equilibria as follows:

$$S_+: \quad \begin{pmatrix} \frac{-\Delta_2+c-a\Delta_1-\sqrt{(\Delta_2+c+a\Delta_1)^2-4ab}}{2} \\ \frac{-\Delta_2-c+a\Delta_1+\sqrt{(\Delta_2+c+a\Delta_1)^2-4ab}}{2a} \\ \frac{\Delta_2+c+a\Delta_1-\sqrt{(\Delta_2+c+a\Delta_1)^2-4ab}}{2a} \end{pmatrix} \tag{10}$$

and

$$S_-: \quad \begin{pmatrix} \frac{-\Delta_2+c-a\Delta_1+\sqrt{(\Delta_2+c+a\Delta_1)^2-4ab}}{2} \\ \frac{-\Delta_2-c+a\Delta_1-\sqrt{(\Delta_2+c+a\Delta_1)^2-4ab}}{2a} \\ \frac{\Delta_2+c+a\Delta_1+\sqrt{(\Delta_2+c+a\Delta_1)^2-4ab}}{2a} \end{pmatrix} \tag{11}$$

or, in a compact form, $S_\pm = (x_\pm, y_\pm, z_\pm)$. Note that either S_+ or S_- represents a group of equilibria.

To discuss the stability of these equilibria, consider the Jacobian of system (8) at these two groups of equilibria:

$$J_\pm = \begin{pmatrix} 0 & -1 & -1 \\ 1 & a & 0 \\ z_\pm & 0 & x_\pm - c \end{pmatrix}.$$

To obtain the eigenvalues of $J_\pm$, consider the characteristic equations:

$$\begin{aligned} f(\lambda) = {} & \lambda^3 + (-x_\pm + c - a)\lambda^2 \\ & + (ax_\pm + z_\pm - ac + 1)\lambda \\ & - az_\pm - x_\pm + c. \end{aligned} \tag{12}$$

By virtue of the Hurwitz criterion [12], all the real parts of the roots λ of (12) are negative if and only if

$$\begin{cases} -x_\pm + c - a > 0, \\ ax_\pm + z_\pm - ac + 1 - \frac{-az_\pm - x_\pm + c}{-x_\pm + c - a} > 0, \\ -az_\pm - x_\pm + c > 0. \end{cases} \tag{13}$$

Consider the following two cases: $S_+ = (x_+, y_+, z_+)$ and $S_- = (x_-, y_-, z_-)$. Notice that $-az_- - x_- + c = -\sqrt{(c + a\Delta_1 + \Delta_2)^2 - 4ab} \leqslant 0$; that is, (13) cannot be satisfied, which implies the instability of all the equilibria in the case of S_-. Thus, we only need to check the stability of the equilibria in the case of S_+ for a given system. All the real parts of the roots of (12) in the case of S_+ are negative if and only if

$$\begin{aligned} & a\Delta_1 + \Delta_2 + c - 2a \\ & \quad + \sqrt{(c + a\Delta_1 + \Delta_2)^2 - 4ab} > 0, \end{aligned} \tag{14}$$

$$\begin{aligned} & ax_+ + z_+ - ac + 1 \\ & \quad - \frac{\sqrt{(c + a\Delta_1 + \Delta_2)^2 - 4ab}}{-x_+ + c - a} > 0, \end{aligned} \tag{15}$$

$$\sqrt{(c + a\Delta_1 + \Delta_2)^2 - 4ab} > 0. \tag{16}$$

Let us check system (1) with parameters setting (2) and (3). Obviously, $(\Delta_2 + c + a\Delta_1)^2 - 4ab > 0$, and therefore, system (1) has equilibria. As mentioned, we only need to check the stability of the equilibria in the case of S_+. With (2), $c > 2a$ and then (14) and (16) hold naturally. However, it is not hard to find that (15) fails to be satisfied after some calculations. Thus, there are no stable equilibria for system (1) with (2) and (3).

In conclusion, we have considered a new chaotic attractor with a striped rectangular shape generated by a Rössler-like system. Some characteristic features of the chaotic attractor has been estimated, and its shape control by simply adjusting suitable parameters has been discussed. From these rich complex phenomena, one can see that a variety of chaotic behaviors can be created via simple feedback control techniques.

References

[1] G. Chen, X. Yu, Chaos Control, Springer-Verlag, Berlin, 2003.
[2] J. Guemez, J. Gutierrez, A. Iglesias, M. Matias, Phys. Lett. A 190 (1994) 429.
[3] K. Pyragas, Phys. Lett. A 170 (1992) 421.
[4] I. Stewart, Nature 406 (2002) 948.
[5] O. Rössler, Phys. Lett. A 57 (1976) 397.
[6] L. Chua, L. Kocarev, K. Eckert, T. Itoh, Int. J. Bifur. Chaos 2 (1992) 705.
[7] G. Chen, T. Ueta, Int. J. Bifur. Chaos 9 (1999) 1465.
[8] M. Yalcin, J. Suykens, J. Vandevalle, Cellular Neural Networks, Multi-Scroll Chaos and Synchronization, World Scientific, Singapore, 2005.
[9] A. Elwakil, S. Ozoguz, M. Kennedy, IEEE Trans. Circuits Systems-I 48 (2002) 531.
[10] A. Wolf, J. Swift, H. Swinney, J. Vatano, Physica D 16 (1985) 285.
[11] P. Muller, Chaos Solitons Fractals 5 (1995) 1671.
[12] W. Hahn, Stability of Motion, Springer-Verlag, Berlin, 1967.